Validation of Myocardial Perfusion Reserve Measurements Using Regularized Factor Images of $H_2{}^{15}O$ Dynamic PET Scans

Frédérique Frouin, Pascal Merlet, Yassine Bouchareb, Vincent Frouin, Jean-Luc Dubois-Randé, Alain De Cesare, Alain Herment, André Syrota, and Andrew Todd-Pokropek

Unité 494, Imagerie Médicale Quantitative, Institut National de la Santé et de la Recherche Médicale, Paris; Service Hospitalier Frédéric Joliot, Département de Recherche Médicale, Direction des Sciences du Vivant, Commissariat à l'Energie Atomique, Orsay; Services de Cardiologie et de Médecine Nucléaire, Centre Hospitalo-Universitaire Henri Mondor, Université Paris XII, Créteil, France; and Department of Medical Physics and Bioengineering, University College London, London, England

The use of $H_2{}^{15}O$ PET scans for the measurement of myocardial perfusion reserve (MPR) has been validated in both animal models and humans. Nevertheless, this protocol requires cumbersome acquisitions such as $C^{15}O$ inhalation or ^{18}F-FDG injection to obtain images suitable for determining myocardial regions of interest. Regularized factor analysis is an alternative method proposed to define myocardial contours directly from $H_2{}^{15}O$ studies without any $C^{15}O$ or FDG scan. The study validates this method by comparing the MPR obtained by the regularized factor analysis with the coronary flow reserve (CFR) obtained by intracoronary Doppler as well as with the MPR obtained by an FDG acquisition. **Methods:** Ten healthy volunteers and 10 patients with ischemic cardiopathy or idiopathic dilated cardiomyopathy were investigated. The CFR of patients was measured sonographically using a Doppler catheter tip placed into the proximal left anterior descending artery. The mean velocity was recorded at baseline and after dipyridamole administration. All subjects underwent PET imaging, including 2 $H_2{}^{15}O$ myocardial perfusion studies at baseline and after dipyridamole infusion, followed by an FDG acquisition. Dynamic $H_2{}^{15}O$ scans were processed by regularized factor analysis. Left ventricular cavity and anteroseptal myocardial regions of interest were drawn independently on regularized factor images and on FDG images. Myocardial blood flow (MBF) and MPR were estimated by fitting the $H_2{}^{15}O$ time–activity curves with a compartmental model. **Results:** In patients, no significant difference was observed among the 3 methods of measurement—Doppler CFR, 1.73 ± 0.57; regularized factor analysis MPR, 1.71 ± 0.68; FDG MPR, 1.83 ± 0.49—using a Friedman 2-way ANOVA by ranks. MPR measured with the regularized factor images correlated significantly with CFR ($y = 1.17x - 0.30$; $r = 0.97$). In the global population, the regularized factor analysis MPR and FDG MPR correlated strongly ($y = 0.99x$; $r = 0.93$). Interoperator repeatability on regularized factor images was 0.126 mL/min/g for rest MBF, 0.38 mL/min/g for stress MBF, and 0.34 for MPR (19% of mean MPR). **Conclusion:** Regularized factor analysis provides well-defined myocardial images from $H_2{}^{15}O$ dynamic scans, permitting an accurate and simple measurement of MPR. The method reduces exposure to radiation and examination time and lowers the cost of MPR protocols using a PET scanner.

Key Words: coronary flow reserve; factor analysis; regularization; $H_2{}^{15}O$ PET scans; coronary artery disease; idiopathic dilated cardiomyopathy

J Nucl Med 2001; 42:1737–1746

The noninvasive assessment of regional myocardial blood flow (MBF) at rest or in response to either exercise or pharmacologic interventions is of great importance in the diagnosis and the evaluation of coronary artery disease (CAD) and other heart diseases. PET is a reliable and noninvasive tool to quantify absolute MBF. Among the different PET tracers that are available to study perfusion, $H_2{}^{15}O$ has major advantages: free diffusion; kinetics independent of changes in myocardial metabolism; and a short half-life (2.1 min), allowing sequential measurements with a low radiation burden for patients. The efficiency of $H_2{}^{15}O$ as a flow tracer has been widely validated in dogs by the microsphere technique (*1*) and in humans by comparative studies with invasive procedures (*2–7*). However, because $H_2{}^{15}O$ is not trapped by myocardial cells, tissue cannot be directly distinguished on the dynamic images. Subtraction of the first images, on which only blood cavities are visible, is unrealistic because of the poor signal-to-noise ratio (SNR) of $H_2{}^{15}O$ dynamic images. This limitation hinders the use of this tracer in clinical routine. $C^{15}O$, which permits labeling of the vascular volume, has been used in combination with $H_2{}^{15}O$ for delineation of the myocardial wall from other anatomic structures (*7,8*) to obtain tissue $H_2{}^{15}O$ time–activity curves suitable for MBF measurements using compartmental analysis (*9*). Another method consists of combining the $H_2{}^{15}O$ bolus technique with a metabolic ^{18}F-FDG study used to define myocardial regions of interest (ROIs) (*3*). The use of FDG appears cumbersome except for com-

Received Feb. 16, 2001; revision accepted Jul. 31, 2001.

For correspondence or reprints contact: Frédérique Frouin, PhD, U494 INSERM, CHU Pitié-Salpêtrière, 91 Blvd. de l'Hôpital, 75634 Paris Cedex 13, France.

bined flow–metabolism studies in patients who have CAD and are being considered for revascularization procedures (*2*,*3*).

Processing of $H_2{}^{15}O$ PET dynamic image sequences with factor analysis methods (*10*,*11*) was proposed to estimate the myocardial factor images directly from dynamic studies (*12*). The limitation of the use of this conventional factor analysis algorithm is the effect of noise in the raw dynamic data on the factor images. To overcome this limitation, another method has been proposed that is close to factor analysis and based on the linear reduction of signal in the sinogram space (*13*). The method requires the introduction of some a priori physiologic information that assumes that the kinetics of the right and left cavities can be derived from the lung kinetics. The myocardial factor image is then reconstructed from the appropriate myocardial sinogram by an iterative reconstruction method. Finally, MBF is estimated by applying the 1-compartment model to time–activity curves resulting from the ROIs that are manually delineated on myocardial factor images. This procedure has recently been validated by comparing, in a group of volunteers and patients, the results obtained by the 2 ways of estimating myocardial ROIs: myocardial factor images and a conventional method that subtracts $C^{15}O$ images from $H_2{}^{15}O$ images (*14*).

This study evaluated an alternative method, based on the spatial regularization of factor analysis of medical image sequences (FAMIS), that was recently proposed (*15*) to improve the quality of factor images for studies with a low SNR. The method applies the conventional algorithm of factor analysis on filtered backprojection reconstructed dynamic series without requiring an a priori physiologic assumption. Regularization of the factor images is the last step of the algorithm. For patients, the new processing method to estimate the myocardial perfusion reserve (MPR) was compared with invasive measurement of coronary flow reserve (CFR) using an intracoronary Doppler technique. For all subjects (patients and volunteers), the MPR obtained from regularized factor images (RFIs) was compared with the MPR obtained from FDG acquisition.

MATERIALS AND METHODS

Study Population

The main characteristics of the population are indicated in Table 1. It included 10 patients (3 women, 7 men; age range, 29–67 y; mean age, 51 y) and 10 healthy volunteers (4 women, 6 men; age range, 30–63 y; mean age, 46 y).

Six of the 10 patients had CAD, as assessed by clinical history and by coronary angiography, and significant stenosis (range, 71%–91%) of the left anterior descending (LAD) artery. None of these 6 patients had a clinical history of, or electrocardiography findings indicating, prior myocardial infarction. Visual and quantitative analysis showed all 6 patients to have normal regional and global angiographic left ventricular ejection fraction, and at the time of examination all were clinically stable and were taking β-blockers, diltiazem, or nitrates.

Four of the 10 patients had had at least 1 episode of acute congestive heart failure related to idiopathic dilated cardiomyopathy. The coronary arteriogram did not show significant stenosis,

TABLE 1
Subject Characteristics, Doppler CFR in LAD Artery, and PET MPR in Associated Anteroseptal Regions

Subject no.	Etiology/% stenosis	EF	Doppler CFR	MPR		
				FAMIS-Op1	FAMIS-Op2	FDG
P1	LAD/75%	61	2.1	1.87	1.96	2.03
P2	LAD/91%	56	1.2	1.39	1.45	1.48
P3	LAD/80%	49	2	2.12	2.01	2.31
P4	LAD/88%	54	1.4	1.12	1.11	1.2
P5	IDC/NS	17	1.7	1.69	1.83	1.59
P6	IDC/NS	18	1.5	1.40	1.26	2.16
P7	IDC/NS	37	1.2	1.13	1.10	1.36
P8	LAD/85%	60	1.2	1.09	1.29	1.48
P9	LAD/71%	66	3	3.34	3.79	2.73
P10	IDC/NS	10	2	1.97	2.11	1.98
C1	None	78	NA	3.36	NA	3.08
C2	None	61	NA	2.06	NA	2.50
C3	None	68	NA	1.97	NA	3.07
C4	None	59	NA	3.32	NA	3.30
C5	None	72	NA	3.81	NA	4.42
C6	None	56	NA	4.93	NA	4.30
C7	None	64	NA	3.43	NA	3.59
C8	None	70	NA	3.55	NA	3.24
C9	None	76	NA	4.43	NA	4.25
C10	None	63	NA	4.84	NA	4.35

EF = ejection fraction; P = patient; LAD = left anterior descending; IDC = idiopathic dilated cardiomyopathy; NS = not significant; C = control; NA = not available.

and no other recognized etiology was evident. At least 1 wk before entering the study, all 4 patients were clinically stable and were taking diuretics and angiotensin-converting enzyme inhibitors.

Ten healthy volunteers having normal echocardiography findings were used as control subjects. They underwent the whole PET procedure but not the Doppler study. These volunteers were age-matched and sex-matched to the patients.

Study Protocol

The Doppler study was performed 1 d before the PET study. Neither clinical modification nor therapy change occurred between the 2 studies. All subjects refrained from oral intake of methyl xanthines, including caffeine, on the day of the studies so as not to diminish the effects of dipyridamole. The protocol was approved by the local ethical committee. Each subject gave informed consent.

Intracoronary Doppler Measurement of CFR. After diagnostic catheterization, an additional dose of 5,000 U heparin was given intravenously, and an 8-French guiding catheter was positioned in the main left coronary artery. The electrocardiogram and mean arterial pressure were monitored continuously. A 3-French Doppler catheter (NuVel; NuMed, Inc., Hopkinton, NY) with a side-mounted crystal of 20 MHz was advanced through the guiding catheter into the proximal segment of the LAD remote to any large branch. The Doppler signal was transmitted to a velocimeter (MDV 20; Millar Instruments, Inc., Houston, TX) and recorded on an ES 1000 recorder (Gould Instrument, Inc., Ballainvilliers, France). The position of the catheter and the range of the sample volume were adjusted to obtain a high-quality signal, as assessed by both audio and graphic controls, and remained unchanged thereafter.

To ensure that the PET measurement of coronary reserve could be performed in similar conditions, no nitrate was injected through the guiding catheter before the Doppler assessment of vasodilator reserve. Dipyridamole (0.80 mg/kg) was infused intravenously at a rate of 10 mg/min. Coronary blood-flow velocities were continuously recorded during the 10 min after the end of dipyridamole infusion. The coronary reserve value was calculated as the mean velocity measured between the fifth and tenth minutes divided by the rest velocity.

After completion of coronary reserve measurement, coronary angiography was performed to evaluate the effect of dipyridamole on coronary artery diameter through a quantitative densitometric analysis of coronary diameter (TSI system; Troütement Synthése Image, Inc., Marne-la-Vallée, France).

PET Acquisition. The subjects were positioned in a TTV03 time-of-flight PET scanner (LETI-CEA, Grenoble, France). Transmission scans were obtained with a retractable ^{68}Ge ring source and used for subsequent attenuation correction of the emission scans. The electrocardiogram was monitored continuously during the examination and 30 min before and 60 min after the PET scan. Blood pressure was measured before injection and every 2 min during the whole examination. The positioning of the heart in the center of the field of view was checked by recording a 5-min transmission scan before the examination. Correct positioning was maintained throughout the study by using laser beams and by marking the skin of the subject's torso.

MBF experiments consisted of intravenous bolus injections of $H_2{}^{15}O$ (11.1 MBq/kg). The experimental protocol included 2 injections with a 20-min delay to allow for ^{15}O decay: one at baseline conditions and another 4–6 min after intravenous injection of dipyridamole (0.80 mg/kg, at a rate of 10 mg/min). Data were acquired in list mode during the 5 min after arrival of the blood radioactivity in the left ventricular cavity.

The subjects finally underwent an FDG PET study. They were given an oral 100-g glucose load 1 h before FDG imaging. After intravenous injection of an FDG concentration of 3.7 MBq/kg, data were acquired in list mode during 60 min.

PET Data Analysis

Image Reconstruction. The $H_2{}^{15}O$ dynamic perfusion studies of 39 scans (15 × 4 s and 24 × 10 s) were reconstructed using a backprojection algorithm with a Hanning filter (cutoff frequency, 0.5 mm^{-1}). Images were corrected for attenuation, random events, dead-time losses, and scattered radiation (*16*). A 20-min static FDG image recorded 40 min after injection was reconstructed using the same procedure. From 2 to 4 consecutive slices were considered for each scan.

Estimation of RFIs. FAMIS was applied to dynamic reconstructed images, according to previously described algorithms (*17,18*), to process the whole set of slices simultaneously. Three factors ($f_1(t)$, $f_2(t)$, and $f_3(t)$, with t being the time variable) and 3 factor images ($a_1(p)$, $a_2(p)$, and $a_3(p)$, with p being the pixels of the images) were estimated from the image sequence. They were associated, respectively, with the right cavities, the lungs and left cavities, and the tissues, including myocardium and liver (Fig. 1).

Once the factors were estimated, the conventional factor images (CFIs) were computed as the least squares solution, which minimized the term E_1 (Eq. 1), representing the squared difference between the raw dynamic data $s(p,t)$ and the combination of the factors $f_k(t)$ and of the factor images $a_k(p)$:

$$E_1 = \sum_{t=1}^{T}\sum_{p=1}^{P}\left(s(p,t) - \sum_{k=1}^{3} f_k(t)\cdot a_k(p)\right)^2. \qquad \text{Eq. 1}$$

The contribution c_k of the kth factor image was defined as the part of the total information that the kth factor image represented in the image sequence such that:

$$c_k = \frac{\sum_{p=1}^{P}\sum_{t=1}^{T} f_k(t)\cdot a_k(p)}{\sum_{l=1}^{3}\sum_{p=1}^{P}\sum_{t=1}^{T} f_l(t)\cdot a_l(p)}. \qquad \text{Eq. 2}$$

Spatial regularization of factor images was achieved using a previously described algorithm (*15*). The method consists in minimizing a criterion E, being the sum of 2 terms. The first term, E_1, represents the adequacy to the raw data, which is minimized by FAMIS; the second term, E_2, introduces some a priori information about the factor images, assuming a regional smoothness of these images. The term E_2 is mathematically defined as follows:

$$E_2 = \mu\cdot\sum_{k=1}^{3}\frac{1}{c_k}\cdot\left[\sum_{p=1}^{P}\sum_{p^*\in V(p)} h_\alpha(a_k(p) - a_k(p^*))\right], \qquad \text{Eq. 3}$$

with h_α being a convex function to account for intensity variation between each pair of neighboring pixels. To avoid a blurring effect at the frontier between adjacent regions, quadratic function is replaced with the following function, h_α:

$$h_\alpha(x) = \begin{cases} -\alpha(2x+\alpha) \text{ if } x \le -\alpha \\ x^2 \text{ if } -\alpha \le x \le \alpha \\ \alpha(2x-\alpha) \text{ if } x \ge \alpha \end{cases}. \qquad \text{Eq. 4}$$

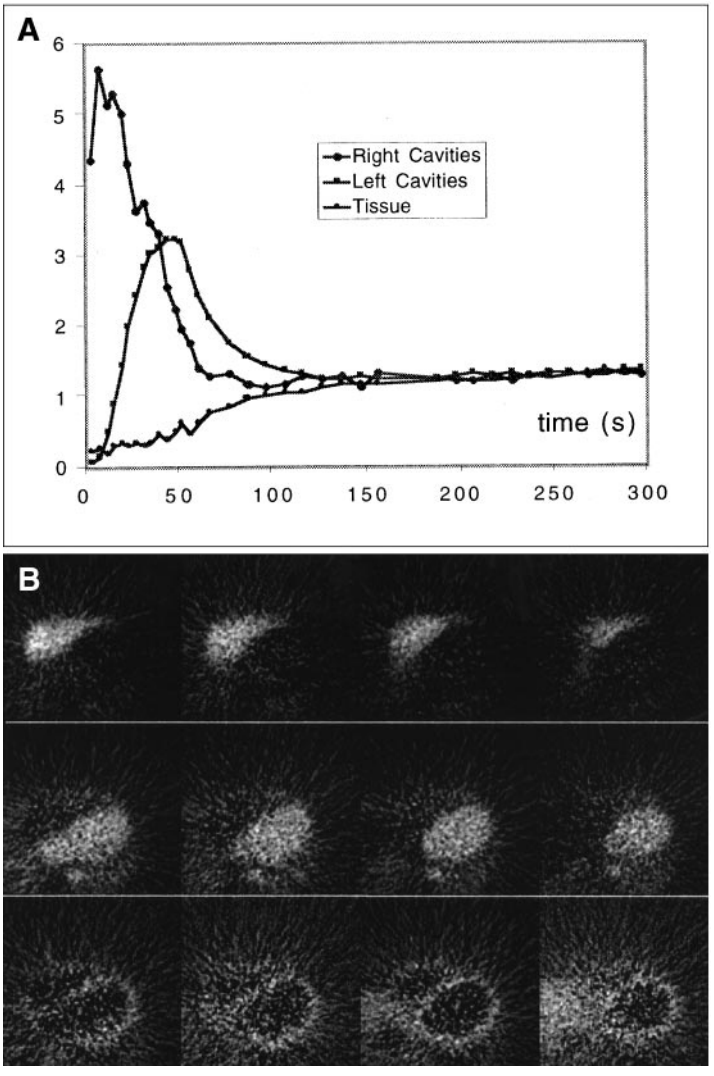

FIGURE 1. Three factors (A) and factor images (B) obtained on 4 consecutive slices for patient with idiopathic dilated cardiomyopathy. First row shows right cavities, second row shows left cavities, and third row shows myocardium and other tissues.

The function h_α is quadratic for small variations in intensity (less than α) and linear for large variations (*15*).

The coefficient μ is set to adjust the trade-off between the fit to the raw data and the a priori information. The 3 terms in Equation 3 corresponding to the 3 factor images are weighted by the inverse of the contribution of each factor image to take into account the lower SNR of the factor images having the smaller contributions.

First trials on simulations showed that the regularization procedure improved factor images from both qualitative and quantitative points of view (*15*). Moreover, there was still some flexibility in the choice of the regularization parameters. The method was applied to real $H_2{}^{15}O$ myocardial studies by determining regularization coefficients from the simulation of a dynamic myocardial PET study (*15*). A value of 0.26 was chosen for the coefficient μ, and the parameter α was set at 1% of the maximum value in the factor images. RFIs were computed slice by slice for each patient on both baseline and stress $H_2{}^{15}O$ studies (Fig. 2).

Extraction of Kinetics. On each slice were drawn ROIs encompassing the left ventricular cavity and the anterior, septal, and lateral myocardial walls. These regions were manually outlined both on FDG images and on RFIs but independently of each other. A 3-color superimposition of the factor images (Fig. 3) was chosen to show complementary structures (i.e., the right and left cavities and the myocardium) on the same figure. The user could adjust the integration of the 3 colors. The graphics software was developed using the Interactive Data Language (Research Systems, Inc., Boulder, CO). Regions were drawn on RFIs resulting from baseline studies and were then reported on RFIs resulting from stress studies to check the accuracy of their location. $H_2{}^{15}O$ time–activity curves were generated for each ROI by reporting the region on the original dynamic series.

Estimation of MPR. For each study, the left ventricular cavity time–activity curve was used as the input function (*19*) and the myocardial time–activity curves were fitted by a 1-compartment model that estimates 3 parameters (rate constants K_1 and K_2 and a spillover fraction, f_v) (*20*). RFIT software (Lawrence Berkeley National Laboratory, Berkeley, CA) was used for this purpose (*21*). The MBF was estimated as the blood-to-tissue transfer rate constant K_1. Regional MPR was estimated as the ratio of peak K_1 to baseline K_1. For comparison with intracoronary Doppler CFR, the MPR was measured in corresponding territories (LAD region) using an ROI encompassing the anterior and septal regions.

Two sets of MPR estimates were obtained: FAMIS-Op1 MPR, which was obtained from the ROIs that were drawn on the RFIs,

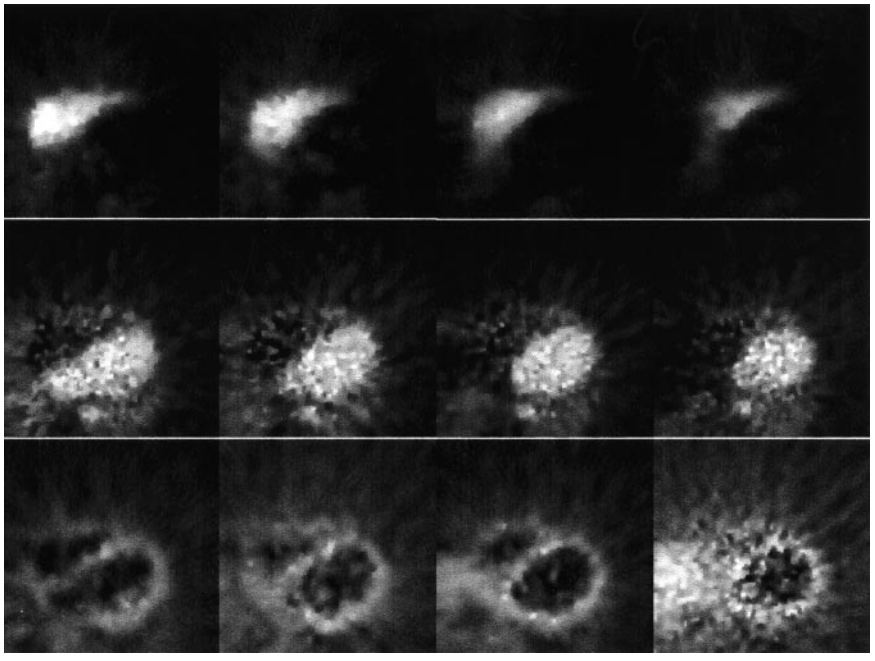

FIGURE 2. RFIs obtained for same patient as in Figure 1, with same layout.

and FDG MPR, which was obtained from the ROIs that were drawn on the FDG scans. A second estimation of MPR (FAMIS-Op2 MPR) was performed by a second operator for patient studies only.

Statistical Analysis

Parameters are expressed as mean ± SD. They were compared using paired or unpaired Student *t* tests when appropriate. A correlation coefficient, assuming a linear regression, was calculated for paired variables. The level of statistical significance was set at 0.05. Bland–Altman representation (*22*) was used to account for the absence of any absolute reference method.

RESULTS

Experimental Results

For the global population, a slight, significant increase in mean arterial blood pressure occurred after dipyridamole infusion when compared with baseline (135 ± 23 mm Hg after dipyridamole and 127 ± 15 mm Hg at baseline). Heart rate increased significantly (88 ± 13 bpm after dipyridamole and 64 ± 12 bpm at baseline). For patients, differences in blood pressure and heart rate between the Doppler and PET examinations were not statistically significant.

No significant change in coronary artery diameter occurred after dipyridamole infusion. Individual measurements of intracoronary Doppler CFR are listed in Table 1. The mean CFR was 1.60 ± 0.33 for patients with idiopathic dilated cardiomyopathy and 1.82 ± 0.70 for patients with LAD stenosis.

CFIs and RFIs were computed systematically. The effect of regularization can be seen by comparing Figures 1 and 2. Table 2 shows the SNRs, which were estimated as the mean value of intensity divided by the SD of intensity, inside each myocardial region of CFIs and of RFIs. In all cases, regularization improved the SNR. The mean relative improvement in SNR (defined as the difference between the SNR of CFIs and the SNR of RFIs divided by the SNR of CFIs) was 70% for the global patient population, 81% for the group with idiopathic dilated cardiomyopathy, and 63% for the

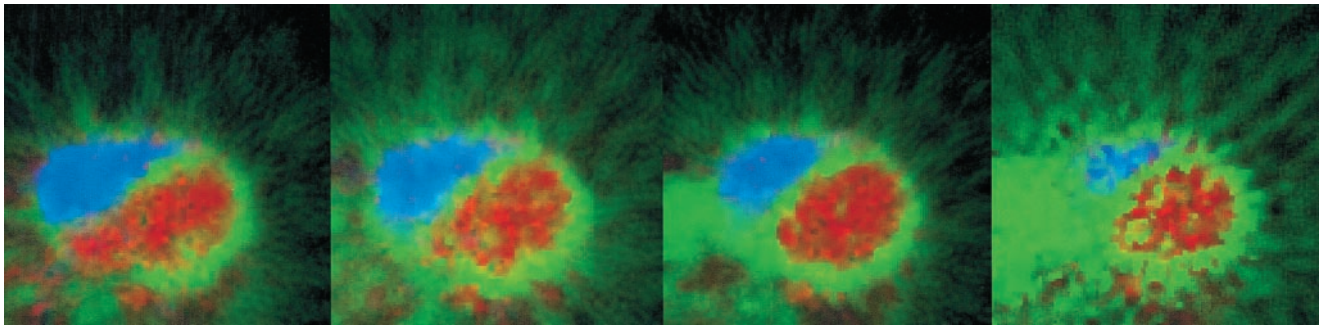

FIGURE 3. Three-color representation of RFIs (blue for right cavities, red for left cavities, and green for myocardium and other tissues) used for manual delimitation of left ventricle and myocardial ROIs.

TABLE 2
SNR of Anterior, Lateral, and Septal Myocardial Regions for CFIs and RFIs

Patient no.	Baseline						Stress					
	Anterior		Lateral		Septal		Anterior		Lateral		Septal	
	CFI	RFI	CFI	RFI	CFI	RFI	CFI	RFI	CFI	RFI	CFI	RFI
1	3.26	5.92	3.15	5.67	3.00	5.43	3.37	5.16	2.67	3.51	3.93	5.66
2	3.77	6.61	3.19	6.59	3.61	6.34	2.59	3.31	2.46	3.17	2.49	3.20
3	2.58	4.93	2.74	4.95	2.68	4.65	2.89	5.18	2.68	4.64	2.28	3.63
4	2.64	3.79	2.17	3.08	2.85	4.19	2.54	4.32	1.95	2.86	2.18	3.27
5	2.17	3.92	2.15	3.77	2.14	3.61	2.05	3.12	1.87	2.76	1.98	2.92
6	2.51	3.98	2.63	3.89	2.31	3.20	2.98	4.52	2.83	4.36	2.74	3.77
7	3.15	6.81	2.69	4.24	2.90	4.38	1.21	1.39	1.61	2.18	1.46	1.67
8	2.47	4.78	1.88	3.22	2.19	3.49	2.10	3.70	2.01	3.45	1.98	3.51
9	2.37	4.28	2.22	3.86	2.36	3.80	1.99	3.15	2.05	2.98	2.41	3.55
10	1.88	3.89	2.20	6.29	1.92	4.13	1.78	5.14	1.92	6.07	1.63	4.65

LAD group. Table 2 shows that the quality of myocardial factor images was generally worse for stress studies; the mean SNR inside myocardial regions of CFIs was 2.59 ± 0.49 for baseline studies and 2.29 ± 0.58 for stress studies. A paired *t* test proved that the difference was significant ($P < 0.005$). Regularization of stress images significantly improved SNR, which was 3.69 ± 1.10 ($P < 0.00001$). However, this SNR remained significantly less than the SNR in baseline RFIs, which was 4.59 ± 1.11 ($P < 0.002$).

For delineation of the left ventricular and myocardial ROIs, the RFIs (and not the CFIs) were used. The operators considered the 3-color display of the cavities and myocardium factor images to be better than the display of the myocardial factor image alone, because myocardial ROIs could be defined while avoiding left and right cavities. In such conditions, the delineation was possible in all cases. Individual MPR values obtained from the anteroseptal region are shown in Table 1. The mean values (±SD) of MPR were 1.55 ± 0.36 for patients with idiopathic dilated cardiomyopathy, 1.82 ± 0.85 for patients with LAD stenoses, and 3.57 ± 1.01 for healthy volunteers. With the second operator, the values were 1.57 ± 0.48 for patients with idiopathic dilated cardiomyopathy and 1.94 ± 0.98 for patients with LAD stenoses.

For delineation of the left ventricular and myocardial ROIs from FDG scans, the static 1-h images were used without reference to the factor images. Individual MPR values obtained from the anteroseptal region defined on the FDG scans are shown in Table 1. The mean values (±SD) of MPR were 1.77 ± 0.36 for patients with idiopathic dilated cardiomyopathy, 1.87 ± 0.59 for patients with LAD stenoses, and 3.61 ± 0.68 for healthy volunteers.

Comparison Between CFR Measurements and Different MPR Measurements

For the 10 patients, 4 sets of reserve values were available (Table 1). Friedman ANOVA by ranks showed no significant difference among the methods of measurement. Results obtained using the RFIs correlated significantly with results obtained using the intracoronary Doppler method (Fig. 4) ($y = 1.17x - 0.30$; $r = 0.97$ for the first operator; $y = 1.35x - 0.54$; $r = 0.95$ for the second operator). The Bland–Altman representation of experimental data (Fig. 5) shows that the discrepancy between RFIs and intracoronary Doppler methods (0.37) was reduced when compared with the discrepancy between FDG and intracoronary Doppler methods (0.57). After removal of the outlier, the discrepancy between FDG and Doppler dropped to 0.42.

Interoperator reproducibility in the definition of ROIs was assessed by comparing MBF in the regions delimited by the 2 operators. No significant difference was found using a Student paired *t* test ($P = 0.88$). Repeatability coefficients were determined using the Bland–Altman approach. They equaled 0.126 mL/min/g for the global analysis including the whole myocardium (0.176 mL/min/g for the regional analysis) in rest studies and 0.38 mL/min/g for the whole myocardium (0.55 mL/min/g for the regional analysis) in stress studies. Repeatability coefficients of MPR were 0.34 (i.e., 19% of mean MPR) for the global myocardium and 0.54 (i.e., 31% of mean MPR) for the regional analysis.

For the 10 healthy volunteers, 2 sets of MPRs were available. No significant difference was found between them. For the global population, a highly significant correlation ($y = 0.99x$; $r = 0.93$) was found between the MPR obtained from RFIs and the MPR obtained from FDG scans (Fig. 6).

Results for both the LAD and the non-LAD regions are given in Table 3 to assess the potential of the method for estimating regional MPR. In healthy volunteers and patients with idiopathic dilated cardiomyopathy, no significant difference was found between the MPR in the LAD regions and the MPR in the non-LAD regions. In patients with LAD stenoses, no significant difference was found between the MPR in the LAD regions and the MPR in the non-LAD regions; however, the mean value of MPR was slightly greater in the non-LAD regions than in the LAD regions (1.94 vs. 1.82).

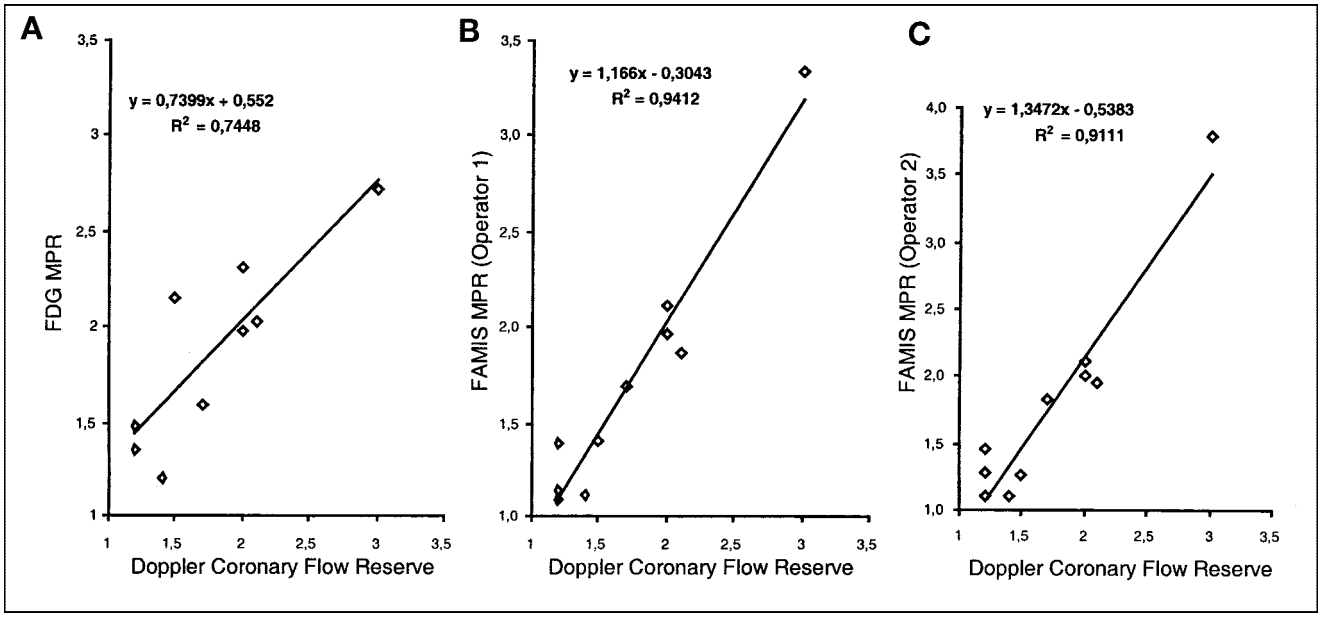

FIGURE 4. Correlation of MPR using either FDG study (A) or $H_2{}^{15}O$ RFI (first operator, B; second operator, C) with CFR using intracoronary Doppler technique.

DISCUSSION

This study validates the use of regularized FAMIS for determining MPR from $H_2{}^{15}O$ dynamic PET scans without additional scanning. This new approach was validated in 2 ways. The first validation was obtained from a study of 10 cardiopathic patients by comparing the MPR with an independent method based on intracoronary Doppler measurements. The second validation was obtained by comparing

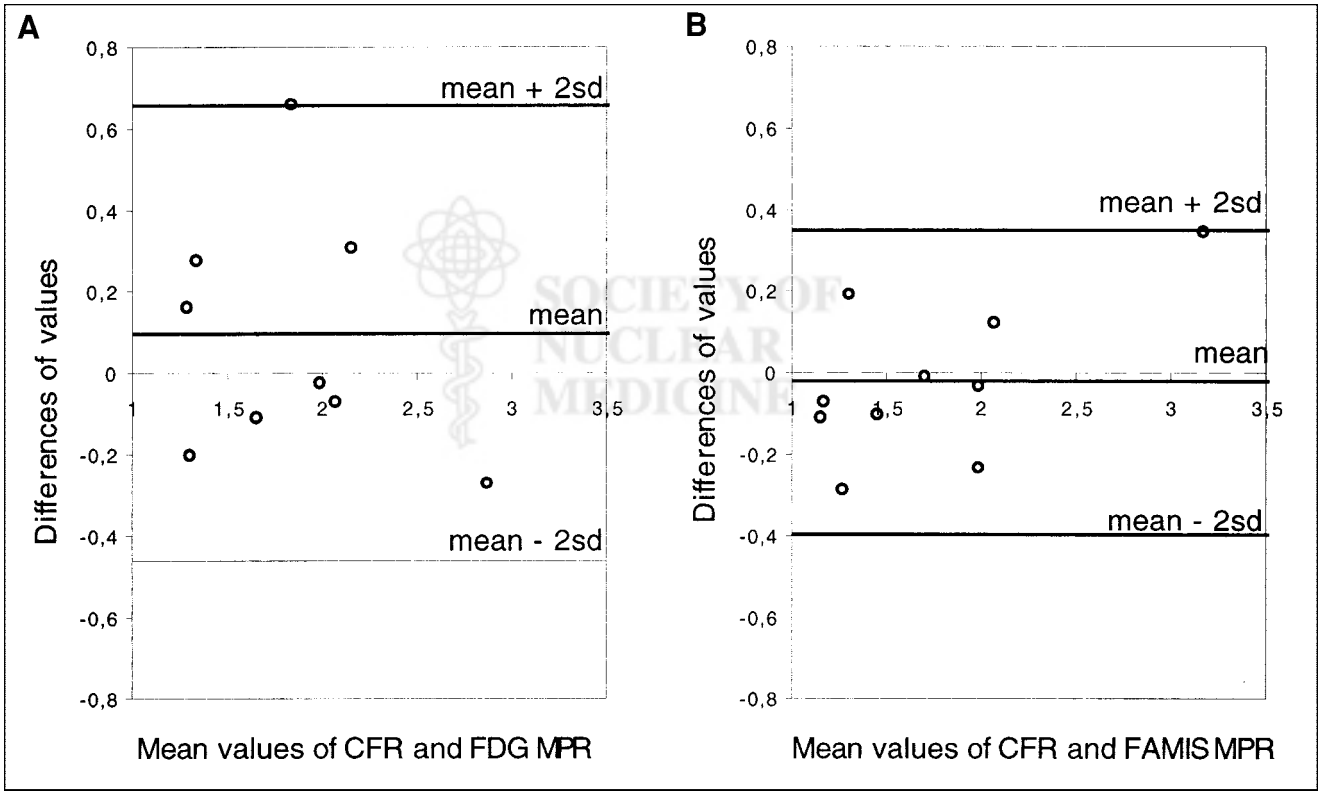

FIGURE 5. Bland–Altman representation of MPR using either FDG study (A) or $H_2{}^{15}O$ RFIs (B) with CFR using intracoronary Doppler technique.

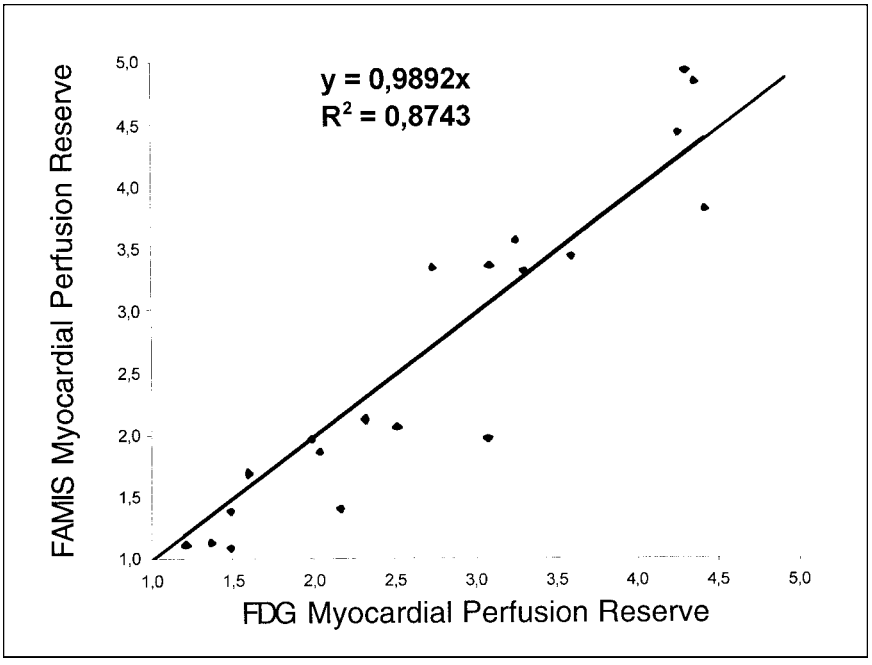

FIGURE 6. Correlation of MPR obtained from $H_2{}^{15}O$ RFIs with MPR obtained from FDG scan.

the MPR obtained from ROIs delineated on the RFIs with the MPR obtained from ROIs delineated on the FDG scan. The MPR values obtained from the RFIs correlated strongly with both the CFR measurements and the MPR values obtained from the FDG scan.

Hermansen et al. (*13*) recently proposed another approach to generate high-quality myocardial factor images. Our method differs in several points. First, we analyzed the reconstructed images, not the sinograms. Second, no a priori physiologic information was required to estimate factors and factor images; in particular, we did not need a model to estimate heart cavity kinetics from lung kinetics. Third, 3 complementary factor images (right cavities, left cavities, and tissue) were generated, and all were useful for delineating myocardial ROIs; indeed, their superimposition avoided the potentially large contamination of myocardial regions by the cavities. Finally, standard and time-efficient algorithms for reconstruction (filtered backprojection) and factor analysis could be used. The main originality of the algorithm presented here was the final regularization of the factor images.

TABLE 3
MPR, Estimated from ROIs Drawn on RFIs, in LAD and Non-LAD Regions

Patient no.	MPR		Control no.	MPR	
	LAD	Non-LAD		LAD	Non-LAD
1	1.87	1.62	1	2.89	3.82
2	1.39	0.98	2	1.52	2.54
3	2.12	1.92	3	3.33	2.37
4	1.12	1.14	4	3.89	4.66
5	1.69	1.76	5	5.39	6.85
6	1.40	1.45	6	5.01	4.85
7	1.13	1.22	7	3.80	2.47
8	1.09	1.31	8	3.50	4.00
9	3.34	4.66	9	5.12	3.00
10	1.97	1.43	10	4.30	5.12

The clinical validation we present supplements clinical validations previously reported (*13*,*14*), which used the method of Hermansen et al. (*13*). Indeed, baseline MBF studies of ischemic patients (*13*) and MPR measurements of volunteers (*14*) have been reported, but not MPR measurements of patients. Moreover, the validation was compared with an independent method, the intracoronary Doppler technique.

For patients with idiopathic dilated cardiopathy, the MPR values (1.55 ± 0.36; range, 1.13–1.97) were close to those published in the literature; a mean value of 1.7 ± 0.21 was recently reported (*23*). For patients with coronary artery stenoses (range, 71%–91%), the mean MPR value was 1.87 ± 0.59 (range, 1.09–3.34). Similar values for patients with coronary artery stenoses have been reported (*24*,*25*). The low MPR values in the reference normal territory (non-LAD region) of CAD patients were already reported (*25*). A possible explanation is that an abnormal flow reserve in angiographically normal territories could represent early functional abnormalities of vascular reactivity (*25*).

Factor analysis was successfully applied to myocardial perfusion PET studies to estimate input function from small hearts using FDG (*26*) and to estimate myocardial factor images with good precision using ^{13}N ammonia (*27*). $H_2{}^{15}O$ studies are more difficult to process because of the low SNR and the free diffusion of the water. Our study shows that regularized FAMIS applied to MBF $H_2{}^{15}O$ studies enabled the generation of high-quality factor images on which myocardium could be delineated accurately and separated from

heart cavities and lungs. During stress studies, the volume of displacement of the myocardium is increased. Because the acquisitions are not gated by the electrocardiogram and the myocardial contraction is larger, the same quantity of tracer is distributed in an apparently larger volume. For this reason, the SNR of dipyridamole factor images is lower than the SNR of baseline factor images. However, regularization, which largely improves the SNR of both baseline and dipyridamole factor images, always makes possible myocardial segmentation.

Although RFIs are useful for the segmentation of the myocardial wall, factors cannot be directly used for the modeling step. Estimated factors are not equivalent to myocardial time–activity curves (Fig. 1), for several reasons. The initial undersampling of pixels in the image sequence (6×6 clusters in myocardial studies) generates mixed kinetics. The aggregation improves SNR in factor estimation, but as a result, the factors are contaminated by each other. Moreover, because only 3 factors are estimated, the lung kinetics are not extracted, and these factors are also contaminated by the lung kinetics. As a consequence, factors and factor images cannot be used directly to extract quantitative information. The myocardial factor image is not strictly equivalent to a tissue blood-flow image, even if the myocardial factor image is related to this blood-flow information.

Uncontaminated kinetics could be estimated by FAMIS using adequate physiologic constraints. Such an estimation would require a complete modeling of the kinetics of the study, including the circulation in the right and left cavities and in the lungs, which is beyond the scope of this article. However, this step is a prerequisite for obtaining RFIs that are of true diagnostic image quality. In this study, the value of the RFIs was assessed only in the crucial step of performing an accurate myocardial segmentation for $H_2{}^{15}O$ studies.

The aim of this study was to estimate MBF or coronary reserve using $H_2{}^{15}O$ dynamic PET scans alone. The advantages of such a modified procedure are obvious and significant: a reduction in the radiation dose to the patient, a shortened acquisition time, and a consequent reduced examination cost. Furthermore, the effects of possible patient motion between the dynamic studies and the supplementary scan are removed. This possible motion results in an error in the positioning of ROIs in the dynamic studies and can explain the larger differences that were observed between FDG and intracoronary Doppler studies.

Different abnormalities have been studied, and the method has proven robust. However, patients with 3-vessel disease that includes large, hypoperfused necrotic territories should be specifically studied and may reveal an intrinsic limitation of the method caused by poor count statistics in $H_2{}^{15}O$ PET scans.

Despite the suggestion that MRI may be used to estimate a coronary reserve index (*28*), the potential field of applications for $H_2{}^{15}O$ PET scans remains wide because PET ensures that absolute values of regional peak and baseline MBF will be determined. Absolute myocardium flow measurements ensure a direct evaluation of MBF reserve that reflects the ability of vasculature to increase flow maximally in response to a hyperemic stimulus. The 2 techniques (PET and Doppler) are not strictly equivalent, because PET measurements are directly related to the myocardium, whereas Doppler measurements are performed on coronary arteries. The absolute quantification of MBF or of MPR can be used in pharmacology trials to measure the impact of drugs. The opportunity to measure MPR noninvasively is an advantage in following up the effect of medical therapy and of major therapeutic interventions, such as revascularization procedures, in ischemic patients. Moreover, with PET, one can simultaneously assess perfusion and metabolism or perfusion and receptor kinetics.

CONCLUSION

$H_2{}^{15}O$ dynamic PET scans with appropriate image postprocessing allowed a noninvasive estimation of MBF. Variability in the determination of MPR was less with RFIs than with the conventional method using FDG scans. Artifacts caused by patient motion between successive scans were suppressed ipso facto. The results of this study suggest that supplementary examinations such as $C^{15}O$ or FDG can be eliminated in MBF and MPR measurement protocols, even for patients with cardiac diseases.

ACKNOWLEDGMENTS

The authors thank Laurence Raynaud and Bernadette Martins for their helpful collaboration. This study was supported by grant 97509 from INSERM and CEA and by the Association Française contre les Myopathies.

REFERENCES

1. Bergmann SR, Herrero P, Markham J, Weinheimer CJ, Walsh MN. Noninvasive quantitation of myocardial blood flow in human subjects with oxygen-15 labeled water and positron emission tomography. *J Am Coll Cardiol*. 1989;1414:639–652.
2. Shelton ME, Senneff MJ, Ludbrook PA, Sobel BE, Bergmann SR. Concordance of nutritive myocardial perfusion reserve and flow velocity reserve in conductance vessels in patients with chest pain with angiographically normal coronary arteries. *J Nucl Med*. 1993;34:717–722.
3. Merlet P, Mazoyer B, Hittinger L, et al. Assessment of coronary reserve in man: comparison between positron emission tomography with oxygen-15-labeled water and intracoronary Doppler technique. *J Nucl Med*. 1993;34:1899–1904.
4. Miller DD, Donohue TJ, Wolford TL, Kern MJ, Bergmann SR. Assessment of blood flow distal to coronary artery stenoses: correlations between myocardial positron emission tomography and poststenotic intracoronary Doppler flow reserve. *Circulation*. 1996;94:2447–2454.
5. Camici PG, Gropler RJ, Jones T, et al. The impact of myocardial blood flow quantitation with PET on the understanding of cardiac diseases. *Eur Heart J*. 1996;17:25–34.
6. Bergmann SR. Clinical applications of myocardial perfusion assessments made with oxygen-15 water and positron emission tomography. *Cardiology*. 1997;88:71–79.
7. Iida H, Yokoyama I, Agostini D, et al. Quantitative assessment of regional myocardial blood flow using oxygen-15-labelled water and positron emission tomography: a multicentre evaluation in Japan. *Eur J Nucl Med*. 2000;27:192–201.
8. Araujo LI, Lammertsma AA, Rhodes CG, et al. Noninvasive quantification of

regional myocardial blood flow in coronary artery disease with oxygen-15-labeled carbon dioxide inhalation and positron emission tomography. *Circulation*. 1991;83:875–885.
9. Kety SS. Measurement of local contribution within the brain by means of inert, diffusible tracers: examination of the theory, assumptions and possible sources of error. *Acta Neurol Scand*. 1965;14(suppl):20–23.
10. Barber DC. The use of principal components in the quantitative analysis of gamma camera dynamic studies. *Phys Med Biol*. 1980;25:283–292.
11. Di Paola R, Bazin JP, Aubry F, et al. Handling of dynamic sequences in nuclear medicine. *IEEE Trans Nucl Sci*. 1982;29:1310–1321.
12. Jamal F, Janier M, Herrero P, et al. Myocardial perfusion assessment with O-15-water using factor analysis [abstract]. *J Nucl Med*. 1996;37(suppl):147P.
13. Hermansen F, Ashburner J, Spinks TJ, Kooner JS, Camici PG, Lammertsma AA. Generation of myocardial factor images directly from the dynamic oxygen-15-water scan without use of an oxygen-15-carbon monoxide blood-pool scan. *J Nucl Med*. 1998;39:1696–1702.
14. Kaufmann PA, Gnecchi-Ruscone T, Yap JT, Rimoldi O, Camici PG. Assessment of the reproducibility of baseline and hyperemic myocardial blood flow measurements with ^{15}O-labeled water and PET. *J Nucl Med*. 1999;40:1848–1856.
15. Frouin F, De Cesare A, Bouchareb Y, Todd-Pokropek A, Herment A. Spatial regularization applied to factor analysis of medical image sequences. *Phys Med Biol*. 1999;44:2289–2306.
16. Trebossen R, Mazoyer BM. Count rate performances of TTV03: the CEA-LETI time-of-flight positron emission tomograph. *IEEE Trans Med Imaging*. 1991;10:165–171.
17. Frouin F, Bazin JP, Di Paola M, Jolivet O, Di Paola R. FAMIS: a software package for functional feature extraction from biomedical multidimensional images. *Comput Med Imaging Graph*. 1992;16:81–91.
18. Frouin F, Cinotti L, Benali H, et al. Extraction of functional volumes from medical dynamic volumetric data sets. *Comput Med Imaging Graph*. 1993;17:397–404.
19. Iida H, Rhodes CG, de Silva R, et al. Use of the left ventricular time-activity curve as a noninvasive input function in dynamic oxygen-15-water positron emission tomography. *J Nucl Med*. 1992;33:1669–1677.
20. Huesman RH, Mazoyer BM. Kinetic data analysis with a noisy input function. *Phys Med Biol*. 1987;32:1569–1579.
21. Huesman RH, Knittel BL, Mazoyer BM, et al. *Notes on RFIT: A Program for Fitting Compartmental Models to Regions-of-Interest Dynamic Emission Tomography Data*. Berkeley, CA: Lawrence Berkeley National Laboratory; 1995:1–9.
22. Bland JM, Altman DG. Comparing methods of measurement: why plotting difference against standard method is misleading. *Lancet*. 1995;346:1085–1087.
23. van den Heuvel AF, van Veldhuisen DJ, van der Wall EE, et al. Regional myocardial blood flow reserve impairment and metabolic changes suggesting myocardial ischemia in patients with idiopathic dilated cardiomyopathy. *J Am Coll Cardiol*. 2000;35:19–28.
24. Di Carli M, Czernin J, Hoh CK, et al. Relation among stenosis severity, myocardial blood flow, and flow reserve in patients with coronary artery disease. *Circulation*. 1995;91:1944–1951.
25. Muzik O, Duvernoy C, Beanlands RS, et al. Assessment of diagnostic performance of quantitative flow measurements in normal subjects and patients with angiographically documented coronary artery disease by means of nitrogen-13 ammonia and positron emission tomography. *J Am Coll Cardiol*. 1998;31:534–540.
26. Wu HM, Huang SC, Allada V, et al. Derivation of input function from FDG-PET studies in small hearts. *J Nucl Med*. 1996;37:1717–1722.
27. Wu HM, Hoh CK, Buxton DB, et al. Quantification of myocardial blood flow using dynamic nitrogen-13-ammonia PET studies and factor analysis of dynamic structures. *J Nucl Med*. 1995;36:2087–2093.
28. Wilke NM, Jerosch-Herold M, Zenovich A, Stillman AE. Magnetic resonance first-pass myocardial perfusion imaging: clinical validation and future applications. *J Magn Reson Imaging*. 1999;10:676–685.

JNM The Journal of NUCLEAR MEDICINE

Validation of Myocardial Perfusion Reserve Measurements Using Regularized Factor Images of $H_2{}^{15}O$ Dynamic PET Scans

Frédérique Frouin, Pascal Merlet, Yassine Bouchareb, Vincent Frouin, Jean-Luc Dubois-Randé, Alain De Cesare, Alain Herment, André Syrota and Andrew Todd-Pokropek

J Nucl Med. 2001;42:1737-1746.

The Journal of Nuclear Medicine is published monthly.
SNMMI | Society of Nuclear Medicine and Molecular Imaging
1850 Samuel Morse Drive, Reston, VA 20190.
(Print ISSN: 0161-5505, Online ISSN: 2159-662X)

SNMMI SOCIETY OF NUCLEAR MEDICINE AND MOLECULAR IMAGING